STUDY OF BENDABILITY OF STEEL SHEETS

Mohamed Ben Bettaieb[1], Xavier Lemoine[2], Laurent Duchêne[1], Anne Marie Habraken[1]

[1] Department ArGEnCo, Division MS²F, University of Liège, Chemin des Chevreuils 1, 4000 Liège, Belgium

[2] ArcelorMittal Research S.A., voie Romaine, F-57238 Maizière-les-Metz, France

ABSTRACT

In the present contribution bending tests are modeled and the bendability of steel sheets is evaluated. Bendability refers to the ratio of the minimum bend radius to the initial sheet thickness at which the bending process is successfully accomplished [1]. The metallurgic microstructure of the studied sheet consists in two principal phases: a fully dense matrix (which may be itself composed by several metallurgic phases) and spherical voids. For that purpose, the Gurson Tvergaard Needleman law ([2], [3], [4]) is used and significantly modified. The behavior of the fully dense matrix is defined by the anisotropic Hill 48 function and the Swift hardening law. The width of the sheet is assumed to be large enough to neglect the transversal strains and the stress component in the thickness direction is also neglected. The bending operation can thus be modelled by a plane strain-plane stress loading. The influence of mechanical parameters such as the initial porosity, the Lankford coefficient and the strain hardening exponent on the bendability is studied herein. The failure here is defined by the onset coalescence of neighbour voids and is checked by using Thomason [5], Pardoen [6] and Brunet [7] coalescence models. So the influence of other phenomena (like the shear band development and the localized necking) on the bendability is neglected here.

Keywords: bendability, Gurson law, semi-analytical model

1. INTRODUCTION

A great deal of experimental evidence indicates that the shear band and the void damage development play co-operative role in promoting bendability of sheets ([8], [9], [10]). The prediction of shear localization requires the use of the finite element method ([11], [12]). In spite of its relevance, the application of this method (especially for non linear, complex behaviors with large deformations and damage aspects) often suffers bad convergence, mesh dependency or loss of ellipticity. It is also time consuming. In order to avoid these problems, analytical or semi-analytical models were developed. These models less general than the finite element method are easily applied on the bending processes only. They don't require a large CPU time and algorithmic developments are minimized but they are unable to take into account the shear band development. In the frame of analytical models, several contributions ([1], [13], [14], [15]) are quoted.

The research goal is to significantly improve the formability prediction in bending processes in order to bring a solution for cases not well taken into account by available criteria (edge effects, strain gradient in the thickness direction…). These improvements require the development of sophisticated behavior laws. They will later be implemented in the finite element code LAGAMINE, developed at the University of Liège for more than 20 years. In order to reach this final goal, the first step of the study consists in the development of a semi-analytical model for the prediction of the bendability of sheets. The kinematic of the bending loading is actually well known and is easy to analytically compute, under some basic assumptions, the strain at each point of the sheet. Once the strain field is known, it is possible to numerically evaluate the evolution of the stress and the dif-

ferent internal variables at the corresponding point of the sheet and eventually to check if critical damage is reached. The purpose of this paper is double: firstly to develop and validate of the chosen behavior law without its incorporation in the finite element code and secondly to evaluate the influence of some mechanical parameters on the bendability of sheets.

2. CONSTITUTIVE EQUATIONS

The set of constitutive equations is defined by the Gurson Tvergaard Needleman (GTN) law ([2], [3], [4]). This law is defined by four principal elements. The first one is the yield function F_p:

$$F_p(\underline{\sigma}, f, \sigma_Y) = \frac{q^2}{\sigma_Y^2} + 2q_1 f \cosh\left(\theta \frac{q_2 \sigma_m}{\sigma_Y}\right) - 1 - q_3 f^2 = 0 \quad (1)$$

In this expression:

- q is the equivalent stress defined by the Hill criterion and equal to $\sqrt{(1/2)\,(\underline{\sigma}_d : \underline{\underline{H}} : \underline{\sigma}_d)}$. Here $\underline{\underline{H}}$ is the Hill matrix and $\underline{\sigma}_d$ is the deviatoric part of the Cauchy stress tensor;
- $\sigma_m = (1/3)\,tr(\underline{\sigma})$ is the mean stress;
- σ_Y is the current yield stress of the fully dense matrix;
- f is the void volume fraction or the porosity;
- q_1, q_2 and q_3: parameters introduced by Tvergaard and Needleman ([3], [4]);
- The coefficient $3/2$ which scales the hydrostatic stress in the initial GTN law is replaced by a coefficient θ to reflect the plastic anisotropy effect of the fully dense matrix;

Many values are used in the literature for the coefficient θ: Ragab et al ([1]) keeps the value of 3/2 used in the initial law. Liao et al. [16] chooses $3\sqrt{(1+2r_0)/6(1+r_0)}$ (r_0 is the Lankford coefficient in the rolling direction). More recently, Benzerga [17] uses a thermodynamic formulation in order to identify this coefficient. And he obtained the following relation:

$$\theta = \left[\frac{8}{5}\left((h_1+h_2+h_3)/(h_1h_2+h_2h_3+h_1h_3)\right) + \frac{4}{5}\left((1/h_4)+(1/h_5)+(1/h_6)\right)\right]^{-1/2} \quad (2)$$

where h_i $(i = 1,...,6)$ are defined as functions of the Lankford coefficients r_0, r_{45} and r_{90} (for more details, see [17]).

This last form of the coefficient θ is adopted in this paper.

The second element of this law is the plastic flow rule defined by the normality relation:

$$\underline{\dot{\varepsilon}}^p = \dot{\lambda} \frac{\partial F_p}{\partial \underline{\sigma}} \quad \begin{cases} \dot{\lambda} = 0 & if\ F_p < 0 \\ \dot{\lambda} \geq 0 & if\ F_p = 0 \end{cases} \quad (3)$$

The third element is the evolution equation of the porosity. This equation derives from approximate incompressibility of the fully dense matrix:

$$\dot{f} = (1-f)\,tr(\underline{\dot{\varepsilon}}^p) \quad (4)$$

The fourth element relates to the hardening function defining the yield stress σ_Y. This function is given by the Swift model:

$$\sigma_Y = K(\varepsilon_0 + \bar{\varepsilon}^p)^n \quad (5)$$

K, n and ε_0 are material parameters and $\bar{\varepsilon}^p$ represents the equivalent plastic strain in the fully dense matrix. The evolution of $\bar{\varepsilon}^p$ is governed by the following equation (6), which was obtained by Gurson by matching the plastic dissipation in the heterogeneous voided material to the plastic dissipation in the homogeneous "equivalent" material:

$$(1-f)\,\sigma_Y\,\dot{\bar{\varepsilon}}^p = \underline{\sigma} : \underline{\dot{\varepsilon}}^p \quad (6)$$

Failure is reached when neighboring voids coalesce. Here the original Thomason model [5] and two of its extensions (by Pardoen [6] and Brunet et al.[7]) are used for modeling the coalescence phase. These models state that no coalescence will occur as long as the following condition is satisfied:

$$\frac{\sigma_1}{\sigma_Y} < \left(\alpha \left(\frac{1}{r} - 1 \right)^2 + \frac{\beta}{\sqrt{r}} \right) \left(1 - \pi r^2 \right) \delta \qquad (7)$$

where σ_1 is the maximal principal stress and r is the void spacing ratio defined as a function of principal strains ε_1, ε_2 and ε_3:

$$r = \sqrt[3]{\left(3f / 4\pi \right) e^{\varepsilon_1 + \varepsilon_2 + \varepsilon_3}} \Big/ \sqrt{e^{\varepsilon_2 + \varepsilon_3} / 2} \qquad (8)$$

Table 1. Different values of α, β and δ

	α	β	δ
Thomason	0.1	1.2	1
Pardoen	$0.1+0.217n$ $+4.83n^2$	1.24	1
Brunet	0.1	1.2	$1-T(\sigma_1/\sigma_Y)$

where T is the triaxiality factor and n is the hardening exponent.

3. NUMERICAL MODELING

3.1. Integration of the 3D GTN law

The integration of the behavior law remains a crucial step in the numerical process especially with material non-linearities and complex behavior. In this frame, many algorithms are developed in the literature. One of the most famous ones is "the elastic predictor-plastic corrector" algorithm. In an incremental formulation, the aim of this algorithm is to decompose the increment of the total strain $\Delta\underline{\varepsilon}$ into an elastic part $\Delta\underline{\varepsilon}^e$ and a plastic part $\Delta\underline{\varepsilon}^p$.

$$\Delta\underline{\varepsilon} = \Delta\underline{\varepsilon}^e + \Delta\underline{\varepsilon}^p \qquad (9)$$

$\Delta\underline{\varepsilon}^p$ can itself be decomposed in the following form:

$$\Delta\underline{\varepsilon}^p = \Delta\varepsilon_{eq}^p \, \underline{n} + tr(\Delta\underline{\varepsilon}^p)\, \underline{I} \qquad (10)$$

where $\Delta\varepsilon_{eq}^p$ is the increment of the equivalent plastic strain, $\underline{n}$ is the unit tensor normal to the yield surface, $tr(\Delta\underline{\varepsilon}^p)$ is the trace of $\Delta\underline{\varepsilon}^p$ and $\underline{I}$ is the identity tensor. The determination of $\Delta\varepsilon_{eq}^p$, $\underline{n}$ and $tr(\Delta\underline{\varepsilon}^p)$ allows computing $\Delta\underline{\varepsilon}^p$ and the complete integration of the behavior law. In the particular case of the classic Von Mises criterion (without damage), the plasticity is assumed incompressible ($tr(\Delta\underline{\varepsilon}^p) = 0$) and the normal $\underline{n}$ is known a priori because it is coaxial to the trial stress. So the only unknown in Eqn. (10) and of the behavior law is $\Delta\varepsilon_{eq}^p$. When the damage is taken into account (Gurson law for example), the assumption of the plastic incompressibility is not valid. So that $tr(\Delta\underline{\varepsilon}^p)$ becomes a new unknown, in addition to $\Delta\varepsilon_{eq}^p$. Aravas treated this case in [18] where he developed an extension of the classic "elastic prediction-plastic correction algorithm" in order to take into account the computation of the trace of the plastic strain (for the von Mises isotropic yield function). In our case, the Hill anisotropic criterion is coupled with the GTN law so the problem is more complicated. Indeed the normal to the yield surface $\underline{n}$ is not coaxial to the trial stress and thus isn't known a priori. It becomes therefore a new unknown to be added to $tr(\Delta\underline{\varepsilon}^p)$ and $\Delta\varepsilon_{eq}^p$. So our development aims to extend the Aravas algorithm to the plastic anisotropy of the fully dense matrix. The main developments of this algorithm are exposed hereafter:

The yield function (1) involves the first and the second invariant of the stress tensor and can be written as:

$$F_p(p, q) = 0 \qquad (11)$$

where p, q are respectively the hydrostatic pressure and the equivalent stress:

$$p = -\frac{1}{3}\underline{\sigma} : \underline{I} \;\; ; \;\; q = \sqrt{(1/2)(\underline{\sigma}_d : \underline{\underline{H}} : \underline{\sigma}_d)} \quad (12)$$

With these notations, the stress tensor can be rephrased as:

$$\underline{\sigma} = -p\underline{I} + 2q(\underline{\underline{H}}^{-1} : \underline{n}) \quad (13)$$

where:

$$\underline{n} = \frac{\underline{\underline{H}} : \underline{\sigma}_d}{2q} \quad (14)$$

Using (12), the flow rule (3) becomes:

$$\Delta\underline{\varepsilon}^p = \Delta\lambda\,(-\frac{1}{3}\frac{\partial F_p}{\partial p}\underline{I} + \frac{\partial F_p}{\partial q}\underline{n}) \quad (15)$$

Eqn. (15) can be written in the following form (see Eqn. (10)):

$$\Delta\underline{\varepsilon}^p = \frac{1}{3}\Delta\varepsilon_p\underline{I} + \Delta\varepsilon_q\,\underline{n} \quad (16)$$

where:

$$\Delta\varepsilon_p = -\Delta\lambda\left(\frac{\partial F_p}{\partial p}\right); \Delta\varepsilon_q = \Delta\lambda\left(\frac{\partial F_p}{\partial q}\right) \quad (17)$$

The elimination of $\Delta\lambda$ in Eqns (17) gives:

$$\Delta\varepsilon_p\left(\frac{\partial F_p}{\partial q}\right) + \Delta\varepsilon_q\left(\frac{\partial F_p}{\partial p}\right) = 0 \quad (18)$$

The elasticity equation gives another form of the stress tensor:

$$\underline{\sigma} = \underline{\sigma}_{prev} + \underline{\underline{C}}^e : \Delta\underline{\varepsilon}^e = \underline{\sigma}^e - \underline{\underline{C}}^e : \Delta\underline{\varepsilon}^p \quad (19)$$

where $\underline{\sigma}_{prev}$ is the stress state computed in the previous increment and $\underline{\sigma}^e$ is the trial stress equal to $\underline{\sigma}_{prev} + \underline{\underline{C}}^e : \Delta\underline{\varepsilon}$.
Using Eqn. (16), we can write Eqn. (19) as:

$$\underline{\sigma} = \underline{\sigma}^e - K\Delta\varepsilon_p\underline{I} - 2G\Delta\varepsilon_q\underline{n} \quad (20)$$

G and K are respectively the elastic shear and the bulk moduli.
Projecting Eqn. (19) onto $\underline{I}$ and $\underline{n}$, and using Eqn. (20), gives:

$$\begin{aligned} p &= -\frac{1}{3}\underline{\sigma}^e : I + K\Delta\varepsilon_p = p^e + K\Delta\varepsilon_p \\ q &= \left(\frac{\underline{\sigma}^e_d.\underline{n}}{2(\underline{n}.\underline{\underline{H}}^{-1}.\underline{n})}\right) - G\Delta\varepsilon_q\left(\frac{\underline{n}.\underline{n}}{2(\underline{n}.\underline{\underline{H}}^{-1}.\underline{n})}\right) \end{aligned} \quad (21)$$

This set of equations is completed by describing the evolution of the state variables (the incremental version of Eqns. (4) and (6)):

$$\begin{aligned} \Delta H_1 = \Delta\bar{\varepsilon}^p &= \frac{-p\,\Delta\varepsilon_p + q\Delta\varepsilon_q}{(1-f)\sigma_Y} \\ \Delta H_2 = \Delta f &= (1-f)\,\Delta\varepsilon_p \end{aligned} \quad (22)$$

In an incremental formulation, the computation algorithm of the integration of the elastoplastic equations reduces to the solution of the set of the non-linear equations ((11), (14), (18), (21) and (22)). These equations are solved using Newton-Raphson method. $\Delta\varepsilon_p$, $\Delta\varepsilon_q$ and $\underline{n}$ were chosen as the primary unknowns, treating Eqns. (11), (14) and (18) as the basic equations in which $p, q, \Delta H_1$ and ΔH_2 are defined by Eqns. (21) and (22).

In case of deformation under plane stress conditions (like the bending process for example) in the plane (x, y), the increment $\Delta\varepsilon_{zz}$ is treated as an extra unknown of the problem, with the extra equation of its determination being the constraint:

$$\sigma_{zz} = 0 \quad (23)$$

The computation algorithm is in principle the same as given previously but with few corrections. Indeed the new Eqn. (23) will be added to the set ((11), (14), (18), (21)

and (22)) and the new unknown $\Delta\varepsilon_{33}$ will be added to the set ($\Delta\varepsilon_p$, $\Delta\varepsilon_q$ and $\underline{n}$).

3.2. Kinematic of the bending operation

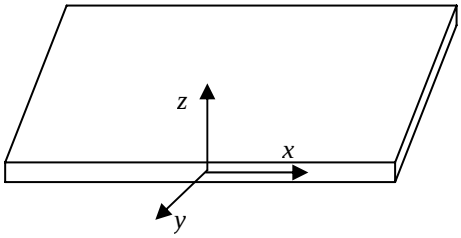

(a)

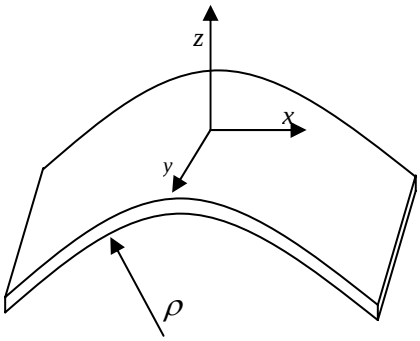

(b)

Figure 1. Geometry of the bended sheet: (a) before bending, (b) after bending

The *1* axis coincides with the neutral axis of the sheet. Under three assumptions, we will define the kinematic of the bending test:

Assumption 1:

The studied sheet is supposed large enough that the strain component ε_{yy} can be neglected.

Assumption 2:

Plane stress state is assumed ($\sigma_{zz} = 0$).

Assumption 3:

The bending is assumed to be pure and the neutral axis is supposed always in the center of the sheet so that the strain component ε_{xx} is defined by the following relation:

$$\varepsilon_{xx} = ln(1 + (z/\rho)) \qquad (24)$$

With these assumptions the stress and the strain tensors are in the form:

$$\sigma = \begin{pmatrix} \sigma_{xx} & 0 & 0 \\ 0 & \sigma_{yy} & 0 \\ 0 & 0 & 0 \end{pmatrix} \quad ; \quad \varepsilon = \begin{pmatrix} \varepsilon_{xx} & 0 & 0 \\ 0 & 0 & 0 \\ 0 & 0 & \varepsilon_{zz} \end{pmatrix}$$

At each increment of curvature $[\rho_i, \rho_{i+1}]$ and at each point of thickness z_i, the increment $\Delta\varepsilon_{xx}$ is known (Eqn. (24)) and by using the numerical algorithm explained previously it is possible to compute the evolution of the different variables and to check if bendability of the sheet is reached.

4. RESULTS

4.1. Material data

In the current paper, the so-called DP 1000 (dual phase) steel was chosen as the fully dense matrix. The material parameters of this steel are given in [13]:

Table 2. Material parameters of DP1000

F	G	H	N
1.051	1.036	0.925	3.182

K	n	ε_0	E	ν
1626	0.17	0.00487	215000	0.3

The values of q_1, q_2 and q_3 are given by [3] ($q_1 = 1.5$, $q_2 = 1$ and $q_3 = q_1^2$) and the value of f_0 is typically used for steel structures ($f_0 = 0.002$).

The thickness of the studied sheet is equal to *2 mm*.

4.2. Results

In this part, the S.I. units are used: σ_{xx} is expressed in *Mpa*, z and ρ are expressed in *mm*. The other numerical data are without unit.

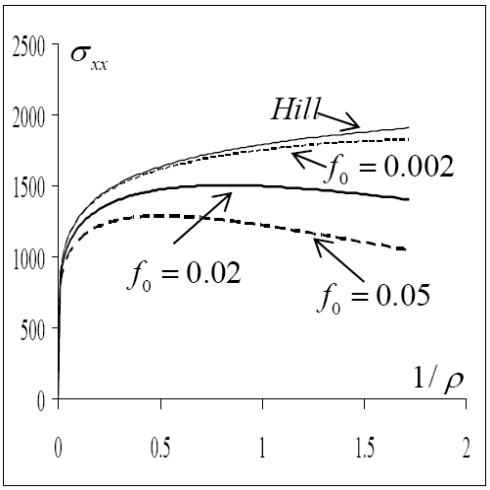

Figure 2. Influence of the initial porosity on the flexural stress

The flexural stress σ_{11} at $z = 1mm$ in terms of the curvature for Hill and GTN material laws is shown in Figure 2. The GTN law is applied for three initial porosities: 0.002, 0.02 and 0.05. It can be observed that if the damage is not taken into account during the simulation, the corresponding σ_{11}-$(1/\rho)$ curve increases constantly. The application of the GTN model leads to a decrease of the predicted σ_{11}-$(1/\rho)$ curves because of the damage evolution. Figure 2 shows also the influence of various level of the initial porosity on σ_{11}-$(1/\rho)$ curves. These curves show that the level of the maximum flexural stress is significantly reduced by the increased presence of voids.

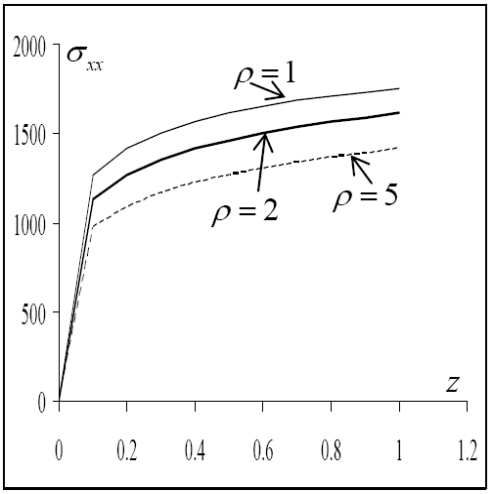

Figure 3. Flexural stress distribution across the sheet thickness

Figure 3 shows that the influence of the curvature on the distribution of the flexural stress through the thickness of the sheet is significant. Indeed σ_{11} increases with decreasing the curvature $1/\rho$. Here only the upper part of the sheet is modeled.

The influence of sheet metal properties namely f_0, n and r_0 are displayed in Figure 4, Figure 5 and Figure 6. The bendability of the studied sheet is reached when the coalescence condition is verified. Here the Thomason, Pardoen and Brunet coalescence model are used to check the bendability. These three models are noted respectively in the following figures *T*, *P* and *B*.

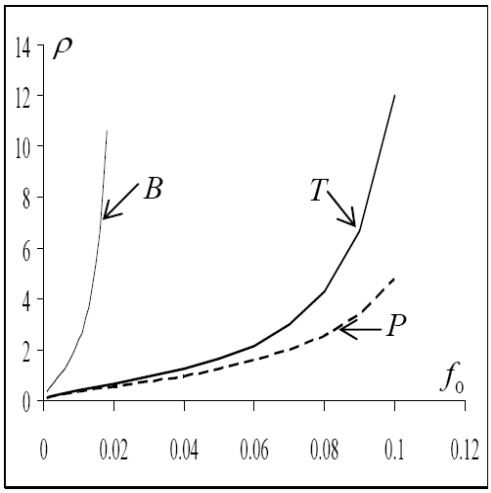

Figure 4. Influence of the initial porosity f_0 on the bendability of the sheet

Figure 4 shows the evolution of the bendability as a function of the initial porosity. For realistic values of f_0 close to that observed in sheet metals (between 0.001 and 0.002), the three coalescence models predict the same bendability. By increasing the value of f_0, the triaxiality factor T increases significantly which decreases the right hand side of Eqn. (7) when the Brunet model (*B*) is applied. For this reason the bendability of the sheet is very limited when the Brunet model is applied with large f_0 values. The difference between the bendability predicted by the initial Thomason model (*T*) and the Pardoen model (*P*) is

due to the difference between the values of parameters α and β for these models.

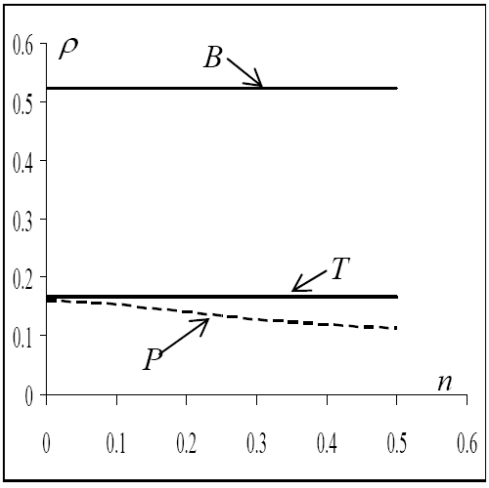

Figure 5. Influence of the hardening exponent n on the bendability of the sheet

Figure 5 shows that there is no influence of the hardening exponent on the bendability when the Thomason or Brunet models are used. Only the application of the Pardoen model is influenced by the hardening exponent. This influence is due to the dependence of the parameter α in Eqn. (7) on n.

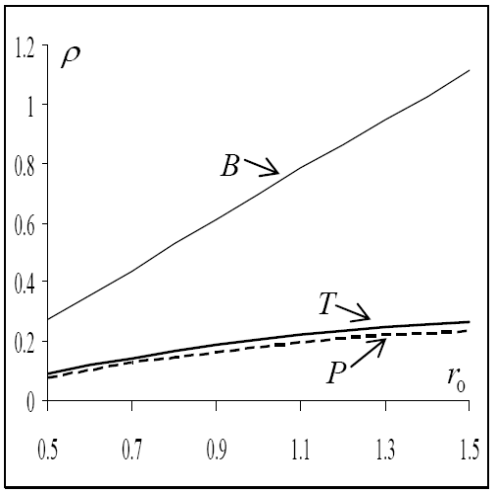

Figure 6. Influence of the Lankford coefficient r_0 on the bendability of the sheet

Figure 6 shows that the plastic anisotropy of the fully dense matrix has a significant influence on the bendability of the sheet. Metal sheets with $r_0 > 1$ possess lower bendability.

Figure 4, Figure 5 and Figure 6 show that there is a significant difference between the application of the different coalescence models in order to evaluate the bendability of sheets. The Brunet model largely underestimates the bendability (especially with higher values of the triaxiality factor T). The difference between the Thomason and the Pardoen models is due to the difference between the value of the parameter α for the two models. The results indicate better bendability with small initial porosities and with low values of r_0.

5. CONCLUSIONS

A numerical algorithm has been developed in order to integrate the GTN law with anisotropic fully dense matrix. This algorithm is an extension of the Aravas algorithm developed for the isotropic case. This algorithm is modified to be able to treat deformation under plane stress condition and is applied to simulate bending processes. This numerical tool is coupled with the Thomason coalescence model (and two of its derivatives) to study the bendability of metallic sheets. The numerical results display the effects of the initial porosity as well as plastic anisotropy. The effect of the hardening exponent is captured by the analytical model when coupled with the Pardoen's coalescence approach to detect the void coalescence. However at this stage, the hardening effect on shear band event is of course not yet taken into account. The whole effect of this parameter on bendability ([1], [14]) needs further steps. A more systematic investigation is planned in order to elucidate the influence of other mechanical and material parameters on the bendability of sheets. In particular, the effect of the kinematic hardening of the matrix and the introduction of the nucleation/growth law developed by Bouaziz [19] will be investigated. After that, the next step is to implement this proposed Gurson model in the Lagamine FE code. This tool will be used to study the combined effect of the void damage development and the occurrence of shear bands.

ACKNOWLEDGMENTS

The authors acknowledge Arcelor-Mittal Research S.A. and the Interuniversity Attraction Poles Program - Belgian State – Belgian Science Policy (P6-24). A.M. Habraken and L. Duchêne also acknowledge the Belgian Fund for Scientific Research FRS-FNRS for its support.

LIST OF REFERENCES

1. Ragab A.R., Saleh Ch.A., "Evaluation of bendability of sheet metals using void coalescence models", Materials Science and Engineering A, vol. 395, 2005, pp. 102-109.

2. Gurson A.L., "Continuum theory of ductile rupture by void nucleation and growth: part I-yield criteria and flow rules for porous ductile media", Journal of Engineering Materials and Technology, vol. 99, 1977, pp. 2-15.

3. Tvergaard V., "Influence of voids on shear band instabilities under plane strain conditions", International Journal of Fracture, vol. 17, 1981, pp. 389-407.

4. Chu C.C., Needleman A., "Void Nucleation Effects In Biaxially Stretched Sheets", Journal of Engineering Materials and Technology-Transactions of the ASME, vol. 102, 1980, pp. 249-256.

5. Thomason P.F., "Ductile fracture of metals". Oxford: Pergamon Press, 1990.

6. Pardoen T., "Numerical simulation of low stress triaxiality ductile fracture", Computers & Structures, vol. 84, Issues 26-27, 2006, pp. 1641-1650.

7. Brunet M., Morestin F., Walter-Leberre H., "Failure analysis of anisotropic sheet-metals using a non-local plastic damage model", Journal of Materials Processing Technology, vol. 170, 2005, pp. 457-470.

8. Akeret R., "Failure mechanism in the bending of aluminum sheets and limits of bendability". Aluminum, vol. 54, 1987, pp. 117–123.

9. Morris L., Kenny L., Ryvola M., "A metallographic examination of the failure of thin sheet during bending". Microstructure Science, vol. 7, 1979, pp 59–67.

10. Steninger J., Melander A., "The relation between bendability, tensile properties and particle structure of low carbon steel". Scandinavian journal of metallurgy, vol. 11, 1982, pp55–71.

11. Kuroda M., Tvergaard V., "Effects of texture on shear band formation in plane strain tension/compression and bending", International Journal of Plasticity, vol. 23, 2007, pp. 244-272.

12. Lievers W.B., Pilkey A.K., Worswick M.J., "The co-operative role of voids and shear bands in strain localization during bending", Mechanics of Materials, vol. 35, 2003, pp. 661-674.

13. Rossi B., Habraken A-M., Frederic P., "On The Evaluation Of The Through Thickness Residual Stresses Distribution Of Cold Formed Profiles", Proceedings of the 10th ESAFORM Conference on Material Forming, Zaragoza, 2007, pp. 570-577.

14. Leu D.K., "A simplified approach for evaluating bendability and springback in plastic bending of anisotropic sheet metals", Journal of Materials Processing Technology, vol. 66, 1997, pp. 9-17.

15. Chakrabarty J., Lee W.B., Chan K.C., "An analysis of the plane-strain bending of an orthotropic sheet in the elastic/plastic range", Journal of Materials Processing Technology, vol. 104, 2000, pp. 48-52.

16. Liao K.L., Pan J., Tang S.C., "Approximate criteria for anisotropic porous ductile sheet metals", Mechanics of Materials, vol. 26, 1997, pp. 213-226.

17. Benzerga A.A., Besson J. , "Plastic potentials for anisotropic porous solids", European Journal of Mechanics-A/Solids, vol. 20, 2001, pp. 397-434.

18. Aravas N., "On the Numerical Integration of a Class of Pressure-Dependent Plasticity Models", International Journal of Numerical Methods and Engineering, vol. 24, 1987, pp. 1395-1416.

19. Bouaziz O., Maire E., Giton M., Lamarre J., Salingue Y., Dimichiele M., "A model for initiation and growth of damage in dual-phase steels identified by X-ray micro-tomography", La revue de métallurgie, 2008, vol. 2, pp. 102-107.